DESIGN OF KEVLAR RADOME FOR MILLIMETER WAVE OBSERVATIONS

A **Thesis Report Submitted to the**

College of Arts and Sciences, Department of Astronomy
University of Virginia • Charlottesville, Virginia

In Partial Fulfillment of the Requirements of the Degree
Bachelor of Science, Astronomy-Physics Major

By

Tryston Raecke
Spring 2021

On my honor as a University student, I have neither given nor received unauthorized aid on this assignment as defined by the Honor Guidelines for Thesis-Related Assignments.

Signature _____ Date _____
Tryston Raecke

Approved _____ Date _____
Bradley Johnson, Department of Astronomy

ABSTRACT

Radomes are structures which serve to protect a central radio detector or antenna from environment damage. Particularly in the case of their use in millimeter wave astronomy, these radomes must endure vacuum pressure while remaining optically transparent in target frequencies. Kevlar, a composite material which exhibits both high optical transparency in millimeter wavelengths and a high Young's modulus, could be a new material of choice in the design of these structures. This paper describes the optical and mechanical requirements of the radome before comparing them against both Kevlar and the current State of the Art. Using simulations with both Python and SolidWorks, Kevlar is shown to outperform these materials by varying degrees. Next, a vacuum test apparatus is designed and fabricated which allows for the physical testing of Kevlar under vacuum. While inconclusive, the nature of this testing suggests that Kevlar adequately responds to the requirements of a radome, specifically when applied to millimeter wave astronomy. Finally, key areas of future work are identified which align with the limitations presented in this study.

I. INTRODUCTION

Millimeter wave astronomy encompasses a swath of research which seeks to answer questions of place and becoming in the universe. As technology improves, so too does humanity's ability to take part in this mode of discovery. Currently, detectors for millimeter wave telescopes are housed in cryogenic vacuum chambers which must be sealed and protected from their outside environment. This form of protection alters the way in which detectors are built and maintained by requiring that the material which covers this opening, the radome, be near transparent in target wavelengths, withstand the mechanical force of atmospheric pressure, and maintain these characteristics across environmental stressors.

Traditionally, radomes come in a variety of materials including ceramics, dielectrics, and metals.[1] Current research seeks to situate a new class of composites into this space. By leveraging the material properties of different epoxy resins and laminates, these composites can take on larger stresses, while remaining comparably thin, so long as the variable nature of resin infusion is limited.[2]

One such laminate of interest is Kevlar. Kevlar is a commercial aromatic polyamide (aramid) fiber which was developed by DuPont beginning in the 1960's.[3] These fibers are heat-resistant and chemically stable, but more importantly, strong. This strength comes as a function of Kevlar's fully extended polymer chains and crystalline packing and can rival the compressive response of aluminum.[4] In outdoor use scenarios, Kevlar must be treated in order to reduce the

[1] Pelton and Munk, "A Streamlined Metallic Radome."
[2] Amsc and CMPS, "Composite Materials Handbook."
[3] Tanner, Fitzgerald, and Phillips, "The Kevlar Story—an Advanced Materials Case Study."
[4] DuPont, "KEVLAR® ARAMID FIBER TECHNICAL GUIDE."

fatigue caused by exposure to ultraviolet light, but ongoing research seeks to suppress this sensitivity.[5]

Previously, Kevlar radomes have been used in military applications due to their low dielectric constants and high mechanical strength in operational ranges between 8 and 10 GHz.[6] For the purpose of millimeter wave astronomy, this would need to be extended to 30-300 GHz, but characterization gaps remain in the literature at this range. In either case, it is expected that Kevlar will remain optically transparent without the need for anti-reflection coatings.[7]

Previously, Kevlar has been combined with Mylar for vacuum windows at CERN where it performed adequately to support a dome with a 7-cm radius of curvature, while only being 0.6-mm thick.[8] Additional simulations of Kevlar's strength alongside Mylar have been used more recently in the design of the SAMURAI spectrometer.[9]

The thesis work presented here seeks to isolate Kevlar composites as an optimal standalone material for the construction of radomes as used in millimeter wave astronomy. Focusing first on the necessary optical requirements, Kevlar is compared against the current State of the Art (SOTA) in radome construction using python scripts. Next, SolidWorks simulations simulate the response of both Kevlar and Ultra-High-Molecular-Weight Polyethylene (UHMWPE) to the mechanical forces of a vacuum. Finally, a vacuum test chamber is designed and fabricated allowing for the physical testing of Kevlar's response to the support of a vacuum.

---

[5] Azpitarte et al., "Suppressing the Thermal and Ultraviolet Sensitivity of Kevlar by Infiltration and Hybridization with ZnO."
[6] Choi et al., "Aramid/Epoxy Composites Sandwich Structures for Low-Observable Radomes."
[7] Datta et al., "Anti-Reflection Coated Vacuum Window for the Primordial Inflation Polarization ExploreR (PIPER) Balloon-Borne Instrument."
[8] Adler et al., "The CPLEAR Detector at CERN."
[9] Shimizu et al., "Vacuum System for the SAMURAI Spectrometer."

II. THEORETICAL BACKGROUND AND PROPOSED METHODOLOGY

A. Optical Loss

As radomes are structures which facilitate microwave transmission, the optics of the material used in its construction are paramount to its use and applicability. In the case of astronomical observations, the target is assumed to be at infinite distance, wherein the incident rays of light are parallel to each other and perpendicular to the planar surface of the detector. Hence, the radome, as a sheet oriented on the x-y plane, can be evaluated in the case of incoming plane waves in the z-direction. This plane wave is given by

$$E_i = E_{i0} e^{-j(\beta - j\alpha)z} \quad (1)$$

where α is the attenuation constant given in Np/m and β is the phase constant of the medium given in rad/m. From this, the complex propagation constant which guides the behavior of the wave through a medium is extracted as [10]

$$\gamma = \alpha + j\beta \quad (2)$$

The depth of penetration as defined as, "the distance in the medium where the magnitude of the penetrating microwave signal reaches 1/e times of its value at the surface of the medium,"[11] is given in meters by

$$\delta = \frac{1}{2\alpha} \quad (3)$$

Solving for α,

$$\alpha = \frac{1}{2\delta} \quad (4)$$

[10] Janezic and Jargon, "Complex Permittivity Determination from Propagation Constant Measurements."
[11] Zoughi and Zonnefeld, "Permittivity Characteristics of Kevlar, Carbon Composites, E-Glass, and Rubber (33% Carbon) at X-Band (8–12 GHZ)."

For values which lack an empirical penetration depth, the attenuation constant can also be derived starting from the complex dielectric constant

$$\hat{\epsilon} = \epsilon' - j\epsilon'' \quad (5)$$

and the loss tangent

$$\tan\delta = \frac{\epsilon''}{\epsilon} \quad (6)$$

From here the complex refractive index and attenuation constant are given as[12]

$$\hat{n} = n - jk \quad (7)$$

$$\alpha = \frac{4\pi\nu k}{c} \quad (8)$$

where ν is frequency and c is the speed of light.

In the case of non-magnetic materials, such as the ones in question here, these values can then be related by

$$\epsilon' = n^2 - k^2 \quad (9)$$

$$\epsilon'' = 2nk \quad (10)$$

Using given values of n, ν, and ϵ', the attenuation constant can then be solved as

$$\alpha = \frac{4\pi\sqrt{2n-\epsilon'}}{c} \quad (11)$$

Using the attenuation constant, one can find the signal after the plane wave passes through a material with,

$$T = T_i e^{-2\alpha t} \quad (12)$$

where T_i is the initial signal and t is the thickness of said material.

From this value, a percentage of signal loss can be calculated which depends only on the depth of penetration and attenuation constant,

[12] Lamb, "Miscellaneous Data on Materials for Millimetre and Submillimetre Optics."

$$\%\, Signal\ Loss = 100(1 - e^{-\frac{t}{\delta}}) \quad (13)$$

Using this value, Kevlar was compared against the current SOTA in radome design.

B. Mechanical Stresses

Radomes are not only optical devices, but inherently structural. Over a span of between 300 and 500 mm, the disk had to withstand a pressure of 1 atm, while optimally deflecting less than 20 mm. This deflection is determined partially by the geometry of the window. A spherical dome, for example, can remain rigid, only susceptible to buckling at a classical buckling pressure of, [13]

$$p_{CL} = \frac{2E}{\sqrt{3(1-\nu^2)}}\left(\frac{t}{R}\right)^2 \quad (14)$$

where E is the Young's modulus, ν is the poisson ratio, R is the radius of curvature, and t is the thickness of the dome.

The downside to this design is that it is much more difficult to manufacture and the mechanism which holds the dome in place much be much stronger than the basic clamps necessary for a flat window. This form of a flat window experiences much greater deflection across its surface with a maximum deflection determined by

$$w_{max} = \frac{3}{16}\frac{p}{E(1-\nu^2)}\frac{R^4}{t^3} \quad (15)$$

where p is the pressure on the window and R is the radius of the dome.

Due to limitations on manufacturing, a 300-mm diameter flat window was decided for the further study of Kevlar with an expected maximum deflection of 19.76 mm when under 1 atm of pressure. A disk shape was explicitly selected due to the load concentrations which occur in non-

[13] Hauviller, "Design Rules for Vacuum Chambers."

circular geometries. Additionally, the ability to evenly clamp the Kevlar becomes more difficult when made non-circular.

To begin to understand the best method by which to simulate the composite structure of the Kevlar, an initial set of SolidWorks simulations were run on uniform disks with diameters of 300 mm. In these simulations, the disks were built from plies of Kevlar-49 & Epoxy with each ply oriented 45 degrees from the one underneath, maintaining symmetry across the entire structure. The forces acting on the disk included gravity and atmospheric pressure with the outside of the disk anchored into place (Figure 1).

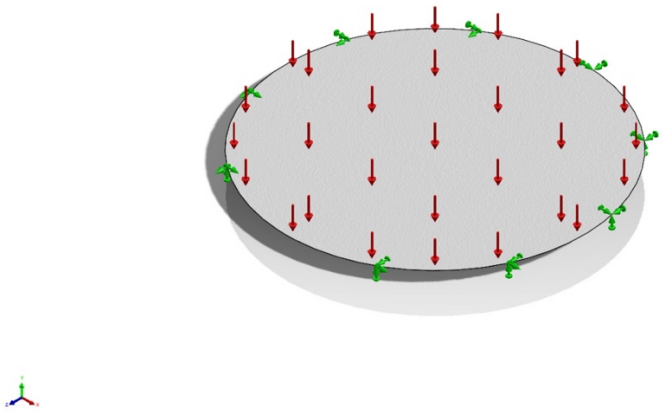

Figure 1. Model of disk with active forces in red and anchors in green

In each case, the maximum displacement was recorded, alongside the Von Mises stress. If the maximum displacement was greater than 20 mm or the von Mises stress exceeded the yield strength of the material at around 1.377e+09 N/m^2, the trial was considered unsuccessful, and the number of plies changed.

This form of testing by plies was later deemed erroneous due to the magnitude of deflection. Instead, a thin feature model was used in further simulations of the Kevlar. This second set of SolidWorks simulations was run on uniform disks with thicknesses of 1.72 mm and 2 mm at 0.7 atm and 1 atm, respectively. They included tests for both Dyneema, a type of unidirectional UHMWPE composite "commercialized in the late 1970s by DSM Dyneema" and Kevlar.[14] Similar to the ply-based simulations, the max displacement was recorded, but now a yield margin of safety given by

$$MS_{yld} = \frac{F_y}{\sigma_V} - 1 \qquad (14)$$

was added where F_y is the yield strength and σ_V is the maximum Von Mises stress. When this value is less than 1, yielding of the material begins which may lead to fracture. Any test was deemed unsuccessful if the displacement was greater than 20 mm and/or deformation was expected to occur.

D. Testing Apparatus Design & Fabrication

To test the Kevlar, a vacuum chamber was constructed which sandwiched the 700-mm diameter Kevlar disk between two 900-mm diameter aluminum plates. The 1" thick base plate had at its center a 1/2-14 NPT through hole for a barbed hose fitting. A central 500-mm hole was cut in this sheet to a depth of 19.05 mm (nominally 3/4"), allowing for a point of flexure of the Kevlar into the cavity. To ensure a vacuum seal was maintained, a O-Ring groove was carved between ~610 and ~618 mm. The exact dimensions of this groove were designed to match a AS568394 O-

[14] Attwood et al., "The Out-of-Plane Compressive Response of Dyneema® Composites."

Ring following guidance from SAE AS5857.[15] In order to secure this portion of the test apparatus to the clamping disk, 16 1/4-20 holes were tapped along a 700-mm ring (Figure 2).

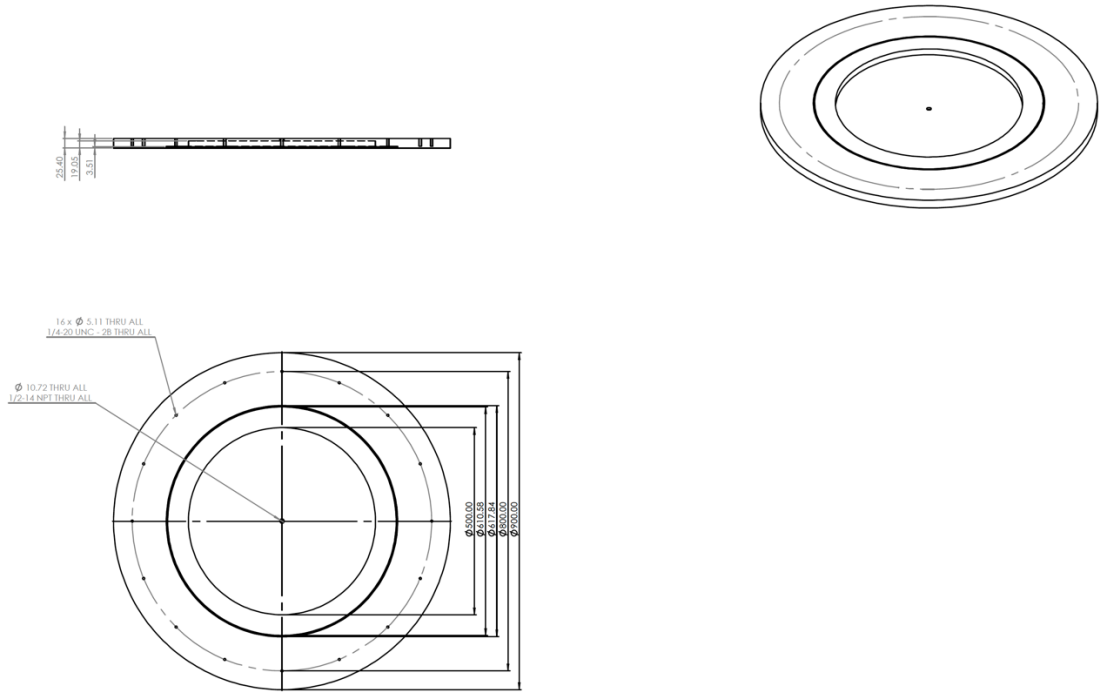

Figure 2. Sketch of base plate for vacuum test chamber

The 0.25” thick clamping ring consisted of a disk with a center cutout of 500-mm. To attach it to the base plate and provide the downward force necessary to squeeze the O-ring, 16 1/4-20 through holes were cut at equidistant points on a 700-mm diameter ring around the center (Figure 3).

[15] Parker Seal Group, *Parker O-Ring Handbook*.

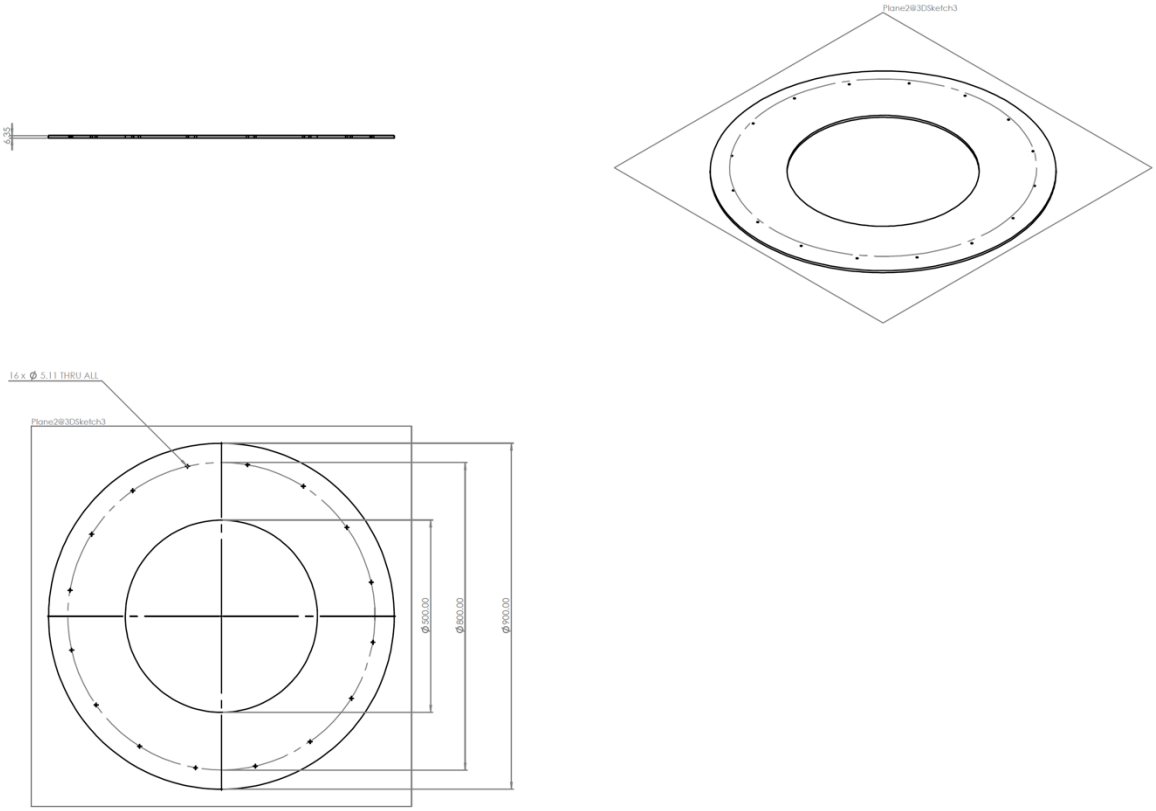

Figure 3. Sketch of aluminum clamp for vacuum test chamber

When assembled, the testing chamber and the Kevlar disk were concentric around the hose fitting (Figure 4).

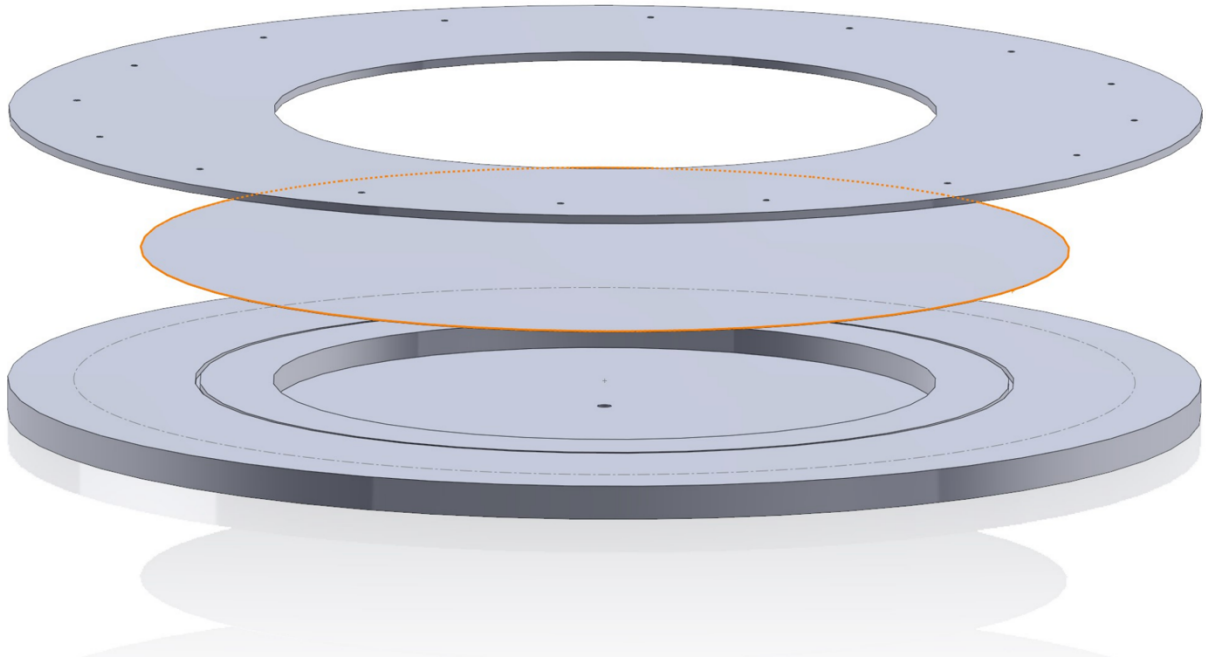

Figure 4. Assembly of vacuum test chamber with (top to bottom) aluminum clamp, Kevlar disk, and aluminum base plate

One this design was complete, fabrication could begin. Starting with a 36” x 36” piece of Kevlar with a thickness of 26 mils, a water jet was used to cut out a properly sized test disk for use in this work. This same water jet was used for bulk cuts on the aluminum. The finer details of the aluminum and the tapped holes were done separately from this process but generally followed expectation (Figure 5).

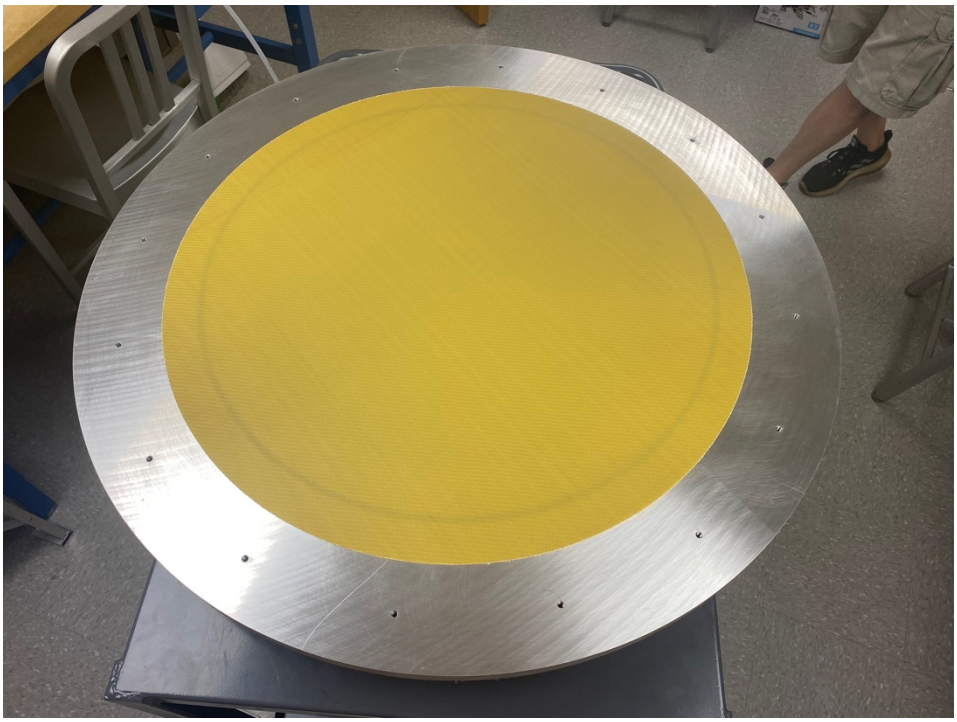

Figure 5. Test apparatus before assembly showing the Kevlar disk sitting on the base plate with a visible O-ring

Once fabricated, the testing apparatus was assembled by first attaching a T-connector to a JB Industries Platinum series vacuum pump (Figure 6). A pressure sensor was attached to one end of the T and calibrated, while a vacuum hose continued out the other and to the hose fitting on the base plate (Figure 7).

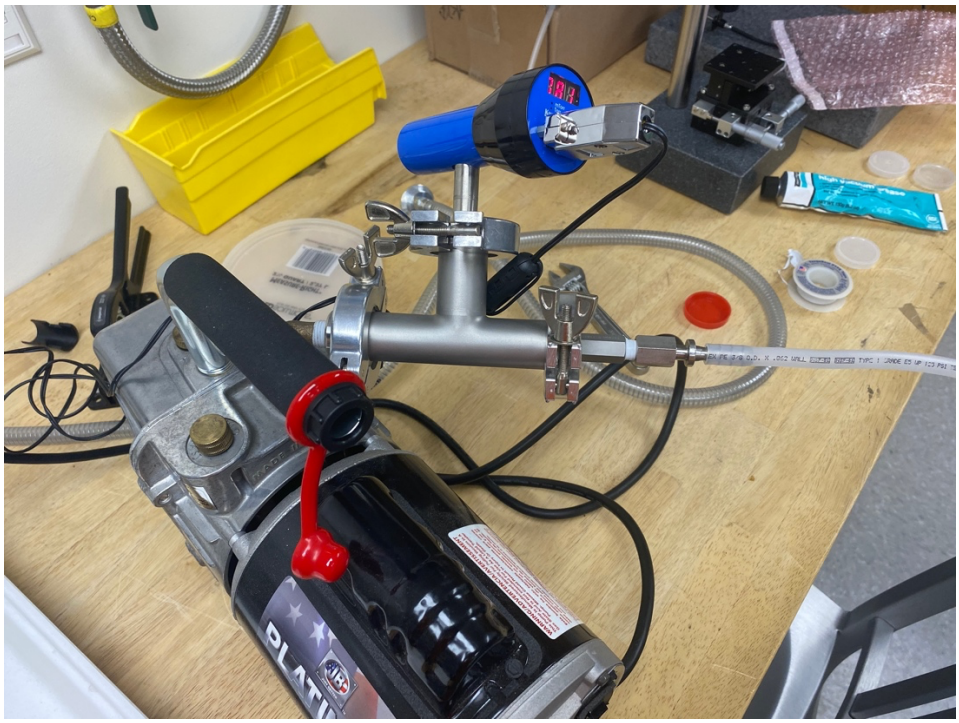

Figure 6. Vacuum pump and pressure sensor used for testing

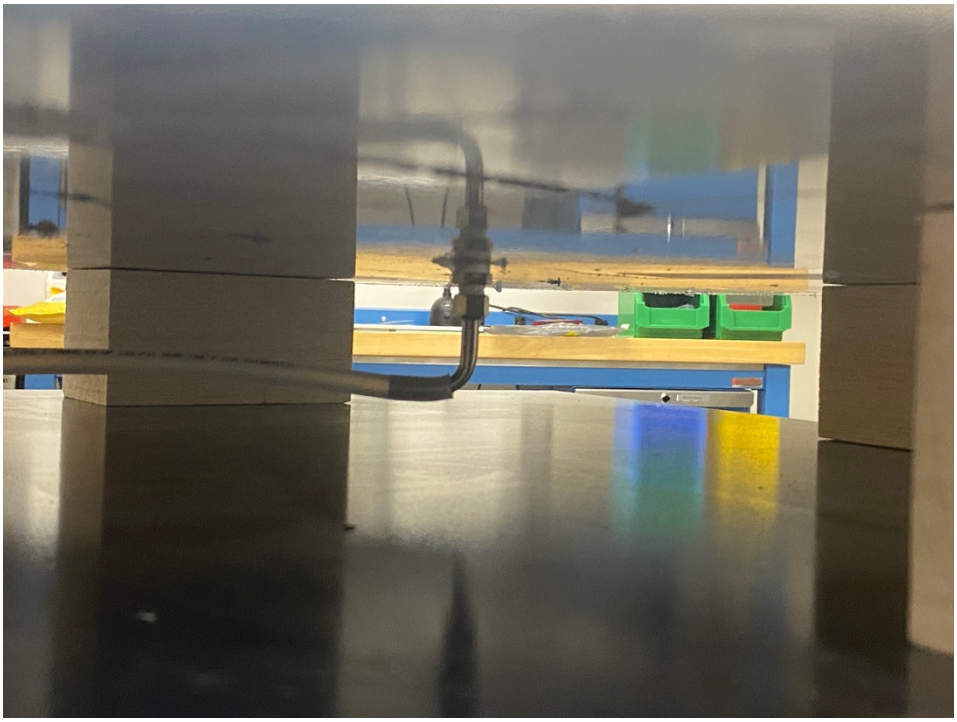

Figure 7. Hose fitting extending from bottom of base plate, which is held by wooden blocks to maintain clearance

Next, the main body of the test apparatus was screwed together in a star pattern to ensure that the O-ring was properly compressed (Figure 8).

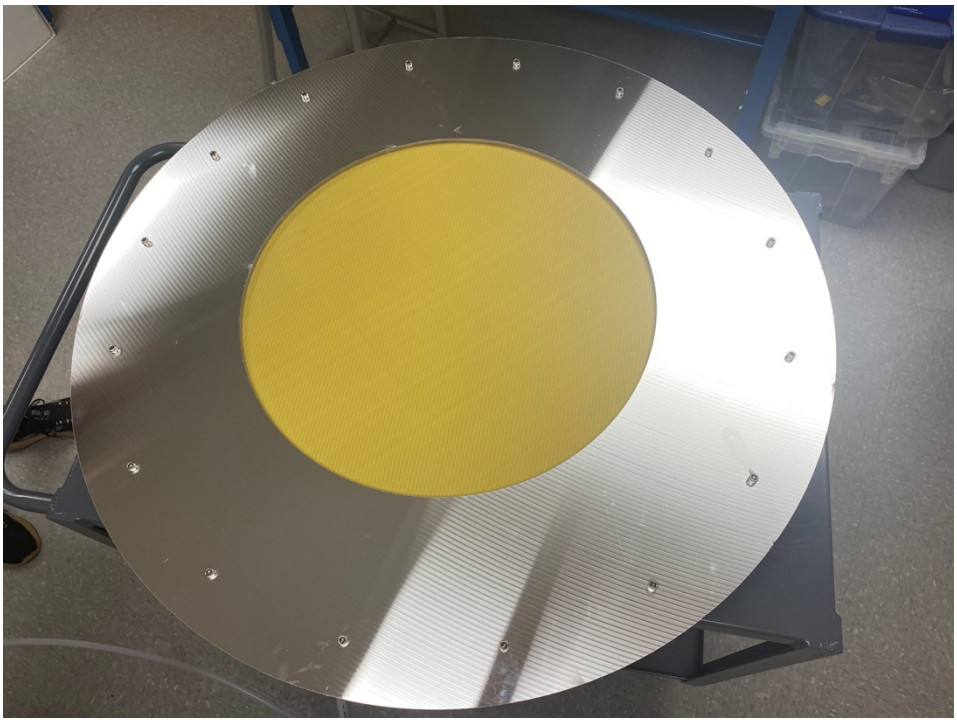

Figure 8. Test apparatus screwed together with Kevlar showing in center

A dial indicator was then attached magnetically to a piece of steel clamped to the outer edge of the aluminum disk. This dial was aligned directly above the hose fitting in the base plate, assuming that location would be the point of greatest deflection (Figure 9).

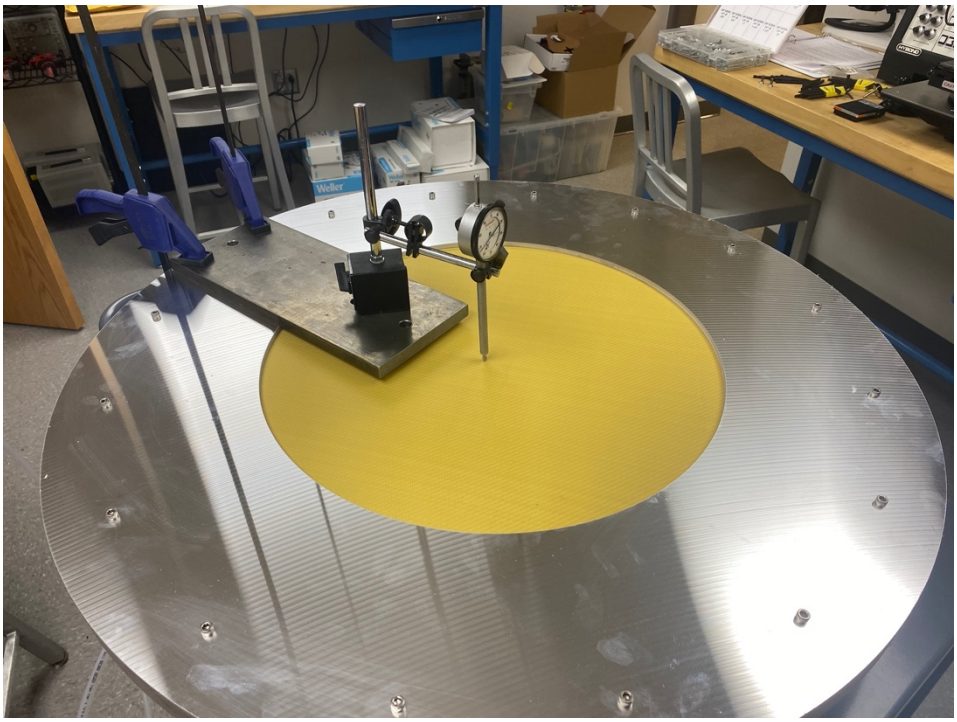

Figure 9. Dial-Indicator zeroed at the center point of the test apparatus

Once everything was in place, the pump was turned on to check the seal of the apparatus. This initial test was deemed successful and the process towards pulling a vacuum in the test chamber continued. The deflection was recorded from the dial indicator as the pressure approached a vacuum as read from the pressure sensor.

III. RESULTS AND DISCUSSION

A. Comparison of Optical Properties Across Kevlar and Current SOTA

In exploring possible materials for the comparison against Kevlar, a suite of the current SOTA was compiled focusing on UHMWPE[16], polyethylene (PE), carbon fiber composite[17], and

[16] Speirs et al., "Design and Measurement of Possible Wide-Band 67-116 GHz ALMA Vacuum Window Anti-Reflection Layers."
[17] Torayca, *T300 Data Sheet*.

glass fiber (E-Glass). The depth of penetration was therefore found in the literature for each material as available (Table 1).

Table 1. Penetration depth of test materials at 10.0 GHz [18]

Material	Penetration Depth [cm]
Kevlar	2.30
Carbon fiber Composite	0.15
E-Glass	1.53

Due to a lack of empirical penetration depths for UHMWPE and PE, different methods were necessary to find the values of the attenuation constant. In the case of UHMWPE, a measurement of the upper limit for the attenuation constant was found at 0.03 ± 0.01 Np/cm.[19] In the case of PE, the alpha value was derived from the values of n, v, and ϵ' as found in the literature (Table 2).

Table 2. Values used in the calculation of the attenuation constant for Polyethylene[20]

v [GHz]	143
n	1.520
ϵ' [F/m]	2.31

[18] Zoughi and Zonnefeld, "Permittivity Characteristics of Kevlar, Carbon Composites, E-Glass, and Rubber (33% Carbon) at X-Band (8–12 GHZ)."
[19] D'Alessandro et al., "Ultra High Molecular Weight Polyethylene."
[20] Lamb, "Miscellaneous Data on Materials for Millimetre and Submillimetre Optics."

Given that most available millimeter wave permittivity research focuses on frequencies between 8.0 and 11.0 GHz, the penetration depth was assumed to be constant between the 10.0 GHz test cases in literature and the target range of 50 - 300 GHz found in this work. While a simplification, the exact nature of this relation was deemed outside the necessary scope here and is the subject of future work. Indeed, the relationship necessary for comparison here should remain the same across all material options given that the alteration of signal frequency changes only the penetration depth and does so similarly across materials.

To compare the different materials, a python script was used to calculate the α and percentage of signal loss across different thicknesses (Appendix I). These plots were then marked with a standard unit thickness of each material as representative of that which would be used in application as a radome (Figures 10-12).

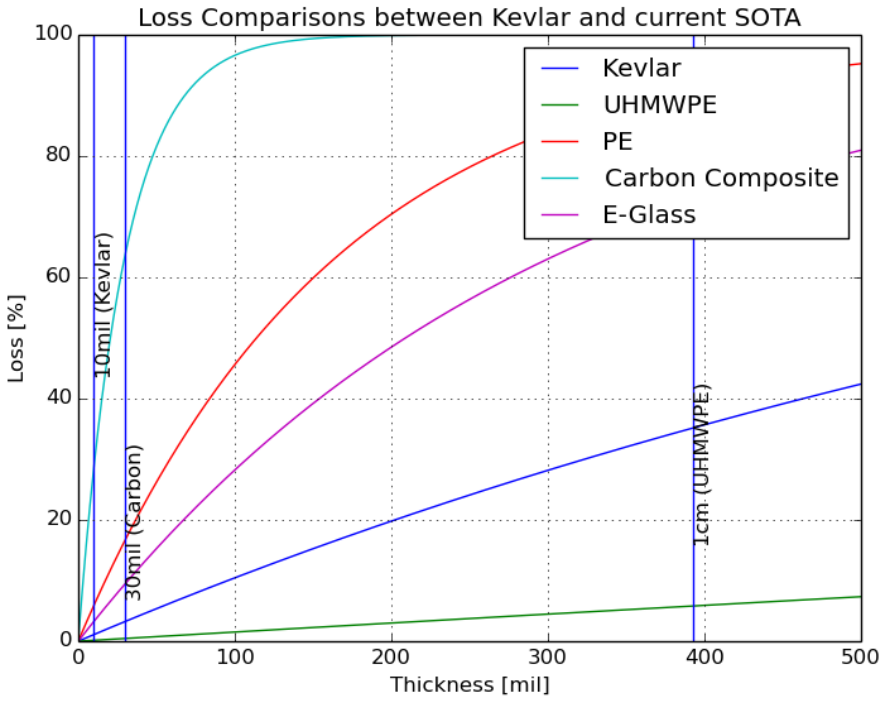

Figure 10. Percent loss comparison of SOTA radome materials with standard unit thicknesses marked for Kevlar, Carbon composite, and UHMWPE

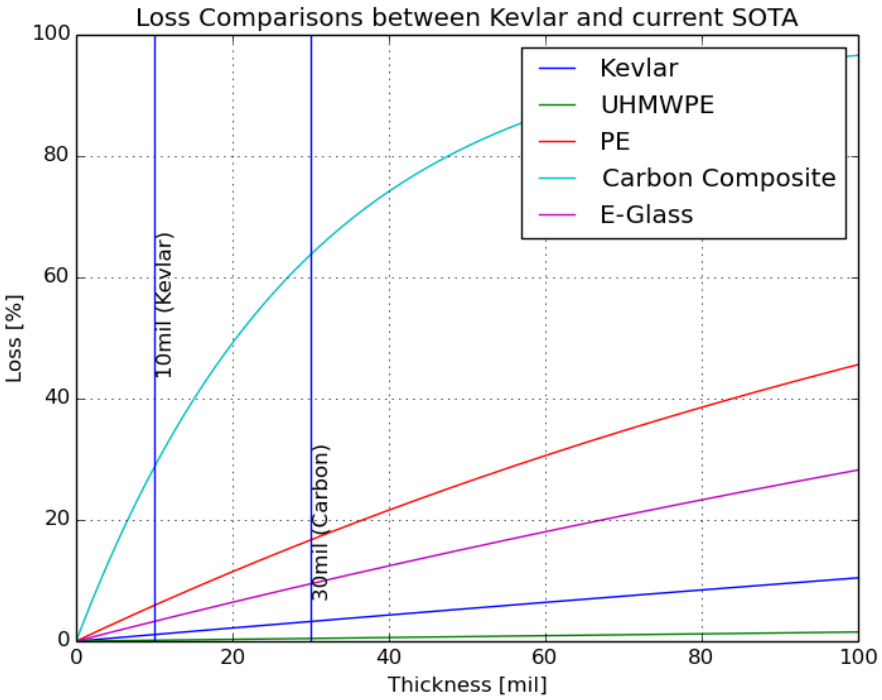

Figure 11. Percentage loss comparison of SOTA materials highlighting differences between 0 to 100 mils

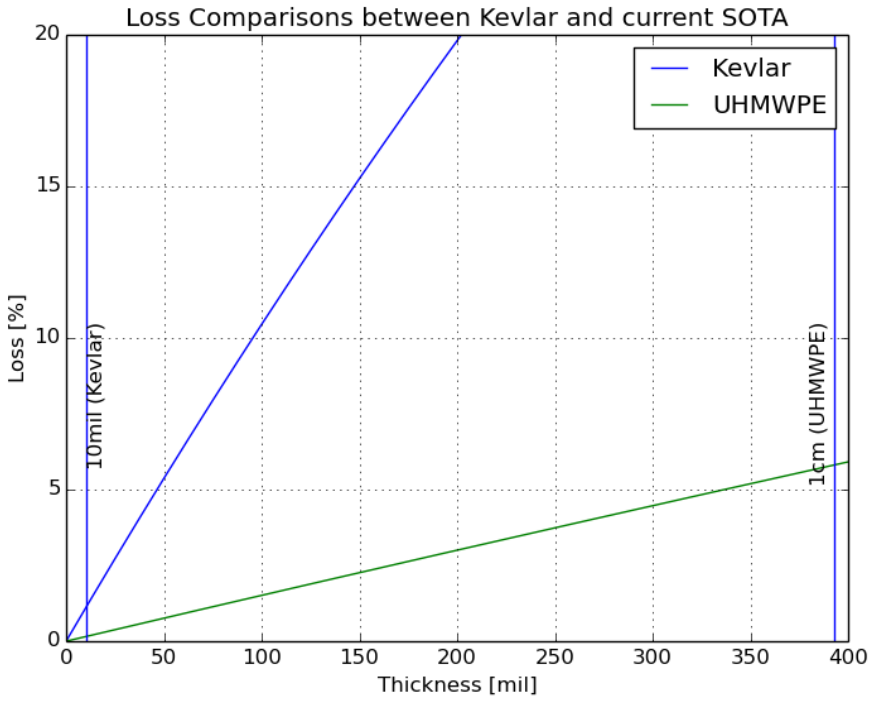

Figure 12. Percentage loss comparisons between Kevlar and the leading composite, UHMWPE

Kevlar shows the lowest percentage of signal loss given the standard thickness of material used. While the slope of the Kevlar loss was greater than that of UHMWPE, the difference in necessary thickness greatly reduces the effective loss in implementation. E-Glass, Carbon Composite, and PE were all deemed non-competitive in this space, but the Carbon Composite was used as an added benchmark for comparison against Kevlar and UHMWPE. Comparatively, Kevlar performed approximately 5.3 times better than UHMWPE and 58 times better than Carbon Composite (Table 3).

Table 3. Comparison of Loss between Kevlar, Carbon Composite, and UHMWPE at the nominal thicknesses of standard use

Material	Standard Thickness [mils]	Loss [%]
Kevlar	10	1.10
Carbon Composite	30	63.77
UHMWPE	393	5.81

B. Mechanical Simulations between Dyneema and Kevlar

The SolidWorks plots for the initial round testing which focused on the number of Kevlar plies can be found in Appendix II. The maximum displacement and von Mises Stresses at each value were far exceeding the requirements or expectations of the work (Table 4).

Table 4. Results of testing Kevlar-49 at different Plies in SolidWorks

Number of Plies	Displacement [mm]	von Mises Stress [N/m^2]
2	9.431e+06	2.465e+08
4	1.189e+06	3.519e+11
10	7.648e+04	9.276e+10
20	9587	2.665e+10
40	1201	7.154e+09

Moving to the second round of simulations which utilized thin feature calculations on a uniform disk, the results began to appear grounded (Appendix III). Following the criteria set out,

only the Kevlar met the yielding and displacement requirements across both pressures and thicknesses (Table 4).

Table 4. Summary results of thin material simulations of Dyneema and Kevlar

Material	Thickness [mm]	Test Pressure [atm]	Max Displacement [mm]	MS_{yld}
Dupont Kevlar 49	2	1	9.338	1.46
Kevlar 49 / Epoxy	2	1	14.01	2.75
Dyneema SK75 Yarn at 175 tex	2	1	10.92	-0.919
Dyneema HB26 [24 ply, 0/90 configuration]	2*	1	44.67	-994
Dupont Kevlar 49	1.72	0.7	10.28	1.59
Kevlar 49 / Epoxy	1.72	0.7	15.42	2.96
Dyneema SK75 Yarn at 175 tex	1.72	0.7	12.02	-0.914
Dyneema HB26 [24 ply, 0/90 configuration]	1.72*	0.7	49.16	-0.994

*The average thickness of the HB26 composite plates is 1.72 mm

C. Vacuum Testing

Once set-up and operated, the test apparatus was largely operating as planned, but once sufficiently low pressure was formed in the chamber, it was noted that the Kevlar appeared to be reaching the bottom of the base plate's recessed region, therefore sealing the hose fitting. Multiple successive attempts were made to test the Kevlar in the now-deemed-limited dynamic range. Each

of these attempts failed, but it was noted that the Kevlar remained strong throughout the process with no show of wear. In many of the trials, when the hose fitting was reached by the Kevlar, the seal was sufficient to require that the entire clamp be unscrewed to release the Kevlar.

IV. CONCLUSION

Across optical and mechanical benchmarks, Kevlar appears to be outperforming other SOTA composites for the purpose of constructing millimeter wave radomes. Without the need for anti-reflective coatings, additional layers of air-tight material, or additional structural support, Kevlar may represent a path forward in the construction of millimeter wave telescopes. While promising, any further research would require both an apparatus with greater dynamic range for vacuum testing and optical tests to ensure that the assumptions of a constant dielectric constant or loss tangent hold up across the target frequencies. Additionally, in order to practically develop and implement the design of a new radome, it is recommended that additional safety tests are taken to cycle the window over operating pressure to ensure that integrity is maintained.[21] The work presented herein represents only an initial wave of testing for Kevlar and future work in the field is highly recommended to check assumptions and ensure safety given the expense and delicacy of astronomy devices. These findings do, however, point towards a new focus of research in the years to come.

[21] Leonhardt and Mapes, "DESIGN OF LARGE APERTURE, LOW MASS VACUUM WINDOWS."

ACKNOWLEDGEMENTS

I would like to thank Professor Bradley Johnson for guiding and mentoring me throughout the thesis process, Peter Dow for machining the finer details of the aluminum, and Sebring Smith for assistance cutting the Kevlar and aluminum.

APPENDIX I. Code for Optical Loss

```
# Plotting Loss [%] of for given thicknesses

import pylab
import numpy as np
import matplotlib.pyplot as plt

# Calculate alpha's in 1/mil
alphakevvert = 1/(4.6 * 394)  # Alpha in 1/mils of kevlar with vertically polarized 10GHz source
alphacarboncompvert = 1/(.15*394)  # Alpha of carbon composite (vertically polarized 10GHz source)
alphaeglassvert = 1/(1.53*394)  # Alpha of E-glass (vertically polarized 10GHz source)
alphaPE = 4*np.pi*(143e9)*np.sqrt((1.520**2)-2.31)/(2.998e8*39370)  # Alpha in 1/mils of PE (@143 GHz) for UHMWPE
alphaUHMWPE = (0.03/393.701)  # UHMWPE converted to 1/mils

# establish tested thicknesses
t = np.linspace(0, 500, 1000)

# Calculate Percentage Loss for each alpha following: T = T_i * e^(-2at)
loss_kevvert = 100-(np.exp(-2 * alphakevvert * t)*100)
loss_cacompvert = 100-(np.exp(-2 * alphacarboncompvert * t)*100)
loss_eglassvert = 100-(np.exp(-2 * alphaeglassvert * t)*100)
lossPE = 100-(np.exp(-2 * alphaPE * t)*100)
lossUHMWPE = 100-(np.exp(-2 * alphaUHMWPE * t)*100)

# Full plot of values
fig = plt.figure(1)
plt.plot(t, loss_kevvert)
# plt.plot(t,loss_kevhoriz)
plt.plot(t, lossUHMWPE)
plt.plot(t, lossPE)
plt.plot(t, loss_cacompvert)
# plt.plot(t,loss_cacomphoriz)
plt.plot(t, loss_eglassvert)
# plt.plot(t,loss_eglasshoriz)
plt.axvline(x=10) # Accent lines for emphasis
plt.text(10.1, 65, "10mil (Kevlar)", rotation=90)
plt.axvline(x=30)
plt.text(30.1, 30, "30mil (Carbon)", rotation=90)
plt.axvline(x=393)
plt.text(393.1, 40, "1cm (UHMWPE)", rotation=90)
plt.legend(["Kevlar", "UHMWPE", "PE", "Carbon Composite", "E-Glass"], loc="upper right")
plt.title("Loss Comparisons between Kevlar and current SOTA")
plt.xlabel("Thickness [mil]")
```

```
plt.ylabel("Loss [%]")
plt.ylim(0, 100)
plt.xlim(0, 500)
plt.grid()

# Zoomed in plot focusing on key test areas
fig = plt.figure(2)
plt.plot(t, loss_kevvert)
# plt.plot(t,loss_kevhoriz)
plt.plot(t, lossUHMWPE)
plt.plot(t, lossPE)
plt.plot(t, loss_cacompvert)
# plt.plot(t,loss_cacomphoriz)
plt.plot(t, loss_eglassvert)
# plt.plot(t,loss_eglasshoriz)
plt.axvline(x=10)
plt.text(10.1, 65, "10mil (Kevlar)", rotation=90)
plt.axvline(x=30)
plt.text(30.1, 30, "30mil (Carbon)", rotation=90)
plt.axvline(x=393)
plt.text(393.1, 40, "1cm (UHMWPE)", rotation=90)
plt.legend(["Kevlar", "UHMWPE", "PE", "Carbon Composite", "E-Glass"], loc="upper right")
plt.title("Loss Comparisons between Kevlar and current SOTA")
plt.xlabel("Thickness [mil]")
plt.ylabel("Loss [%]")
plt.ylim(0, 100)
plt.xlim(0, 100)
plt.grid()

# lot focusing on Kevlar and UHMWPE
fig = plt.figure(3)
plt.plot(t, loss_kevvert)
plt.plot(t, lossUHMWPE)
plt.axvline(x=10)
plt.text(10.5, 10, "10mil (Kevlar)", rotation=90)
plt.axvline(x=393)
plt.text(380, 10, "1cm (UHMWPE)", rotation=90)
plt.legend(["Kevlar", "UHMWPE"], loc="upper right")
plt.title("Loss Comparisons between Kevlar and current SOTA")
plt.xlabel("Thickness [mil]")
plt.ylabel("Loss [%]")
plt.ylim(0, 20)
plt.xlim(0, 400)
plt.grid()

plt.show()
```

APPENDIX II. Results of Testing for Kevlar Plies

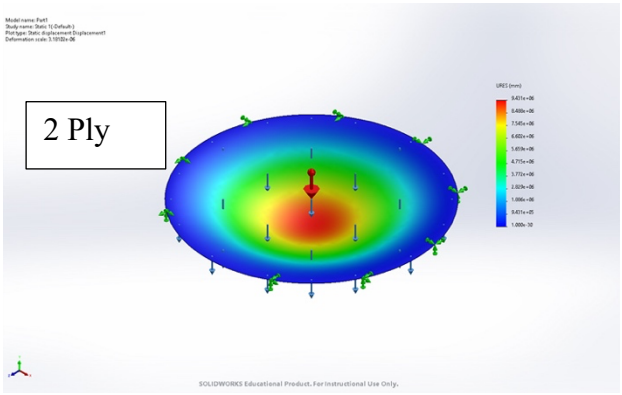

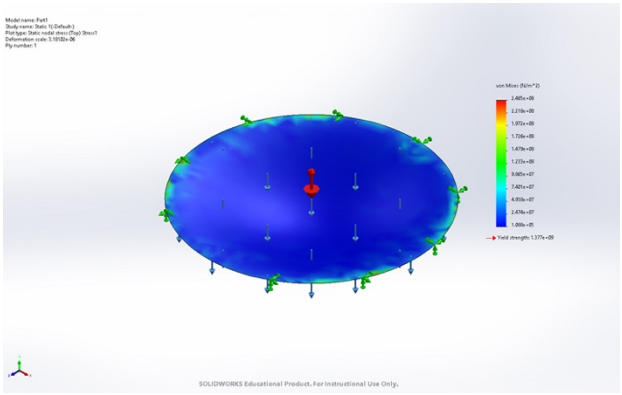

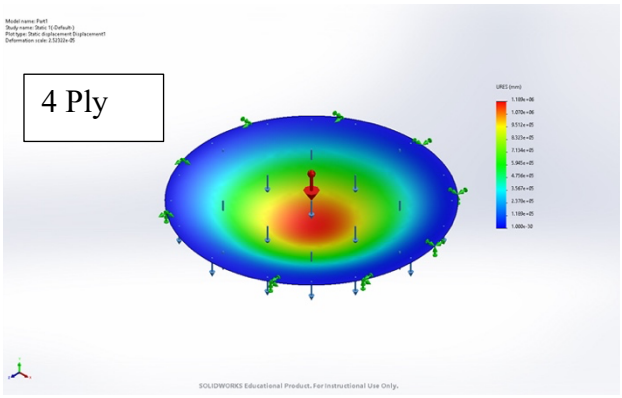

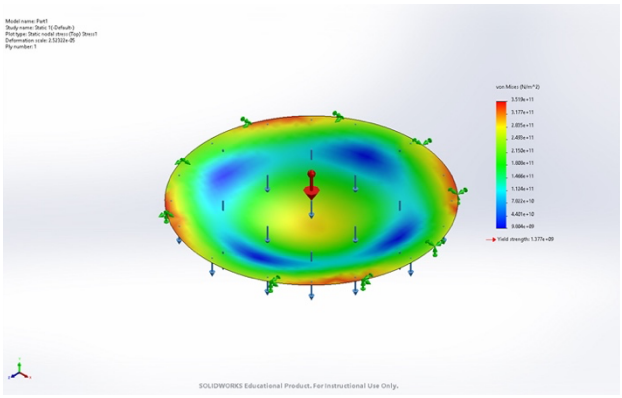

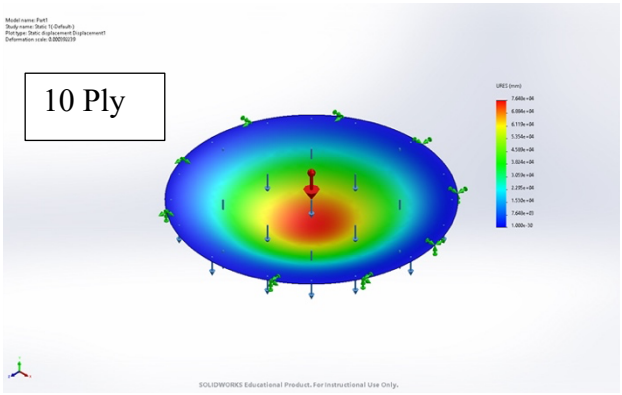

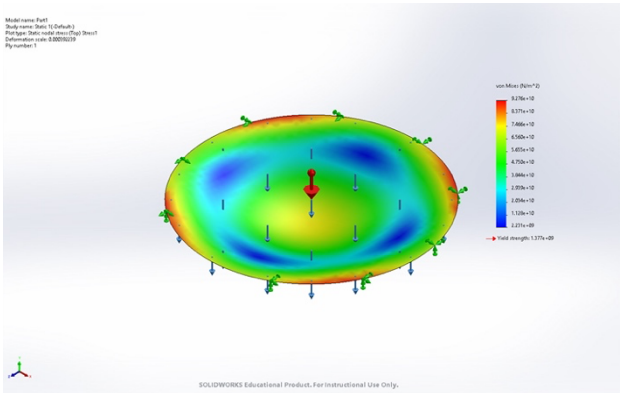

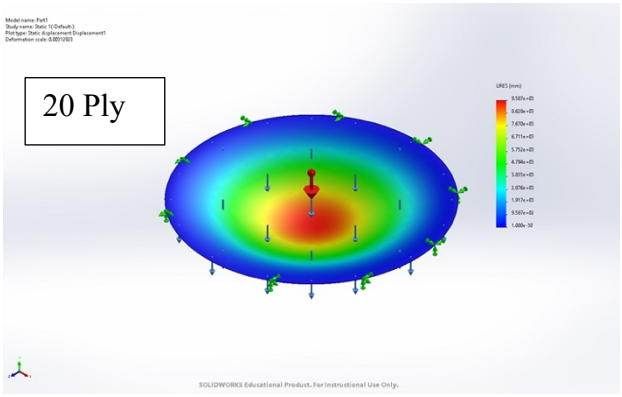
20 Ply
SOLIDWORKS Educational Product. For Instructional Use Only.

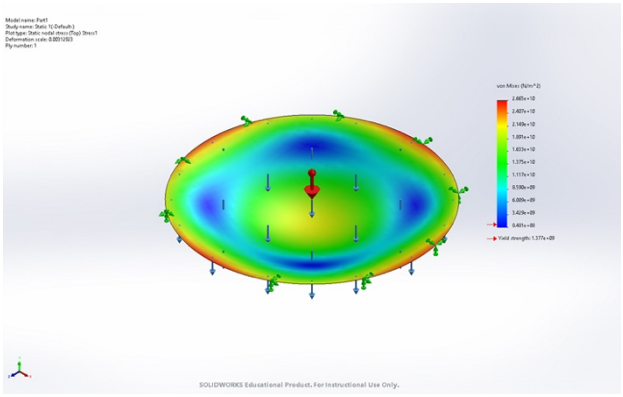
SOLIDWORKS Educational Product. For Instructional Use Only.

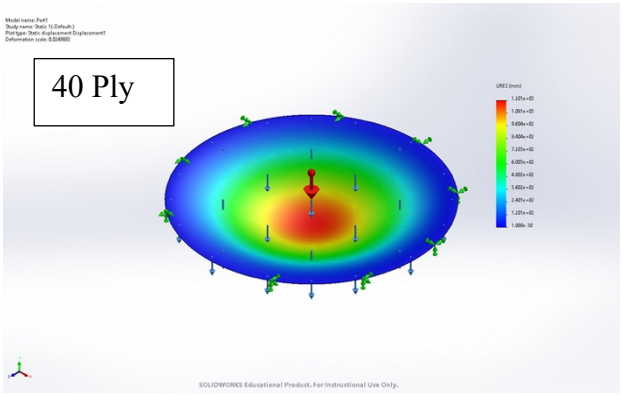
40 Ply
SOLIDWORKS Educational Product. For Instructional Use Only.

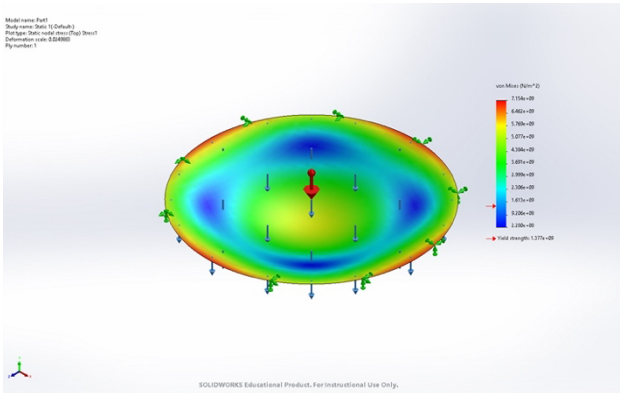
SOLIDWORKS Educational Product. For Instructional Use Only.

APPENDIX III. Results of Thin Feature Simulations for Kevlar and Dyneema variants

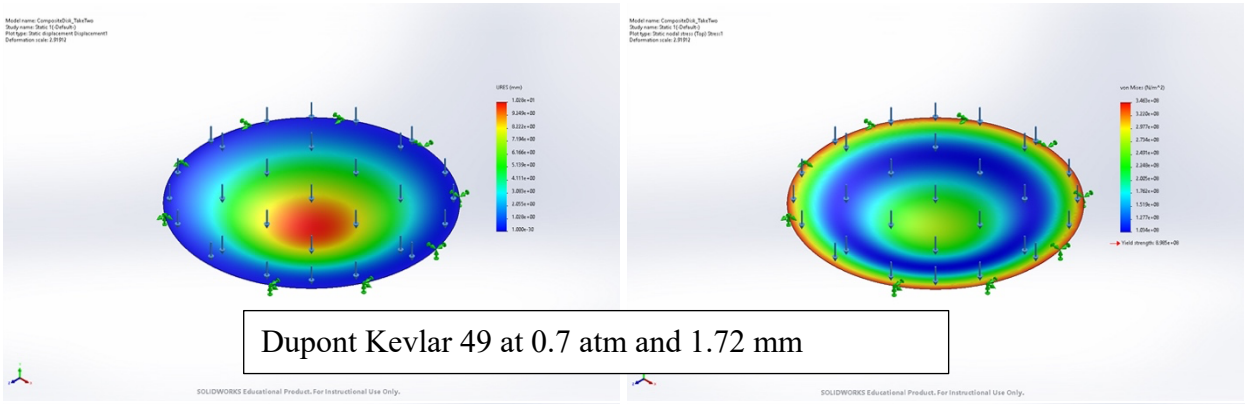

Dupont Kevlar 49 at 0.7 atm and 1.72 mm

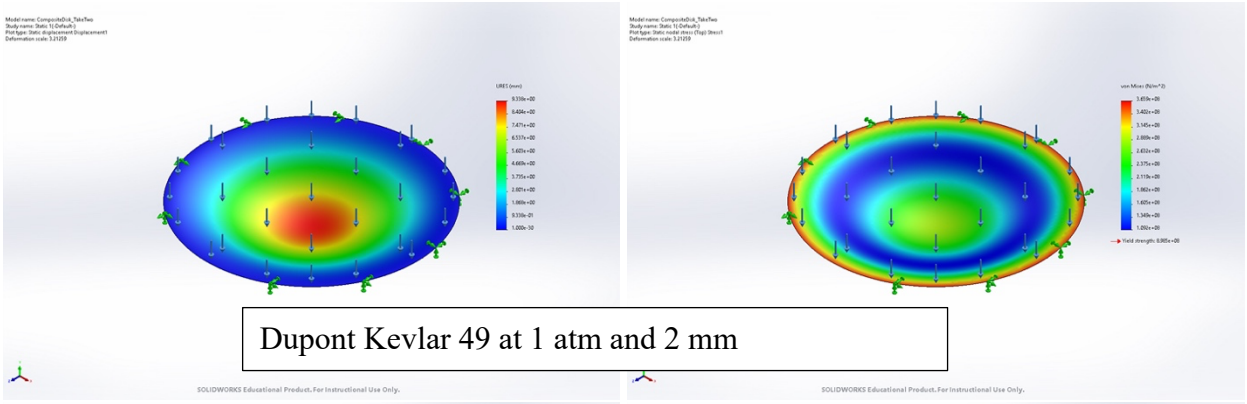

Dupont Kevlar 49 at 1 atm and 2 mm

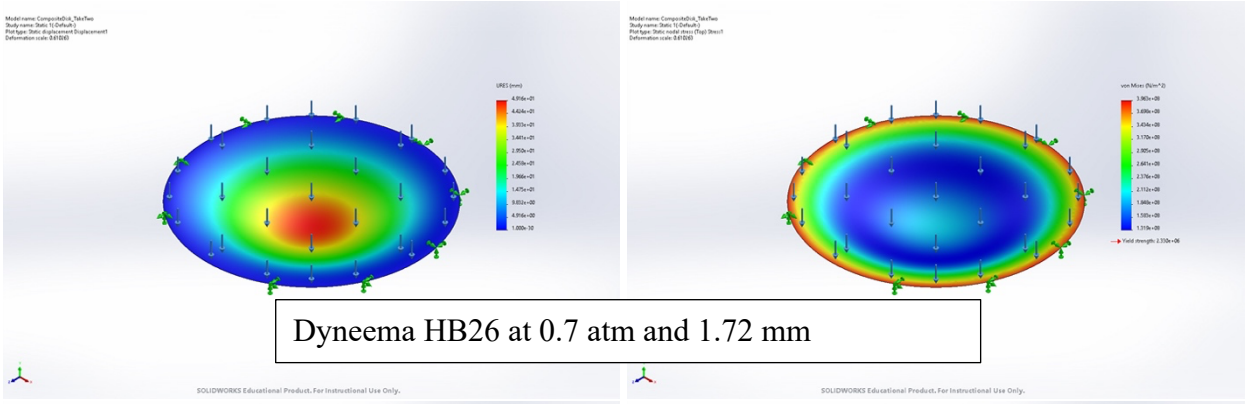

Dyneema HB26 at 0.7 atm and 1.72 mm

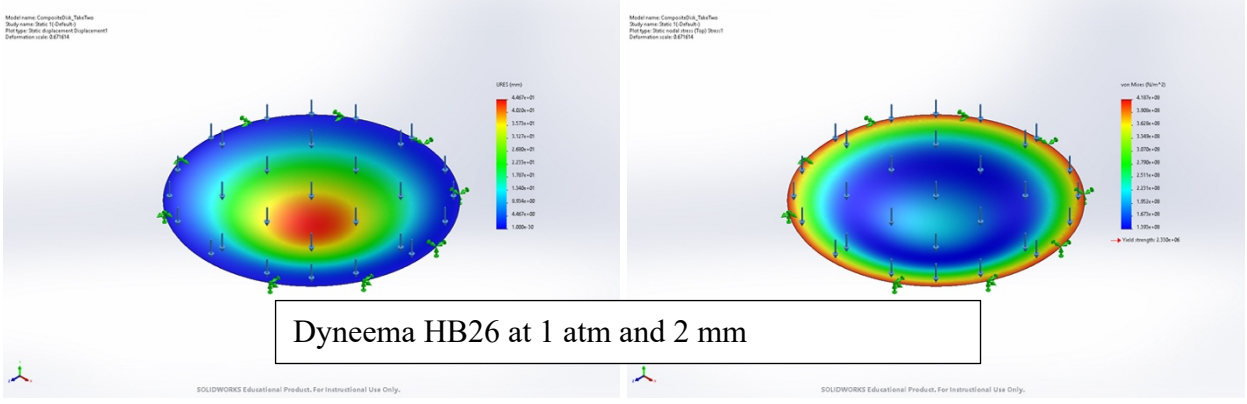

Dyneema HB26 at 1 atm and 2 mm

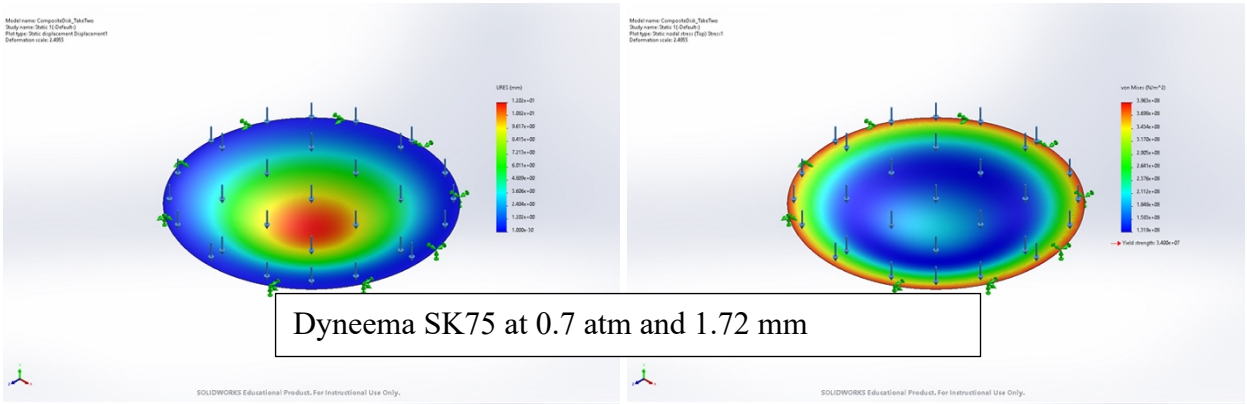

Dyneema SK75 at 0.7 atm and 1.72 mm

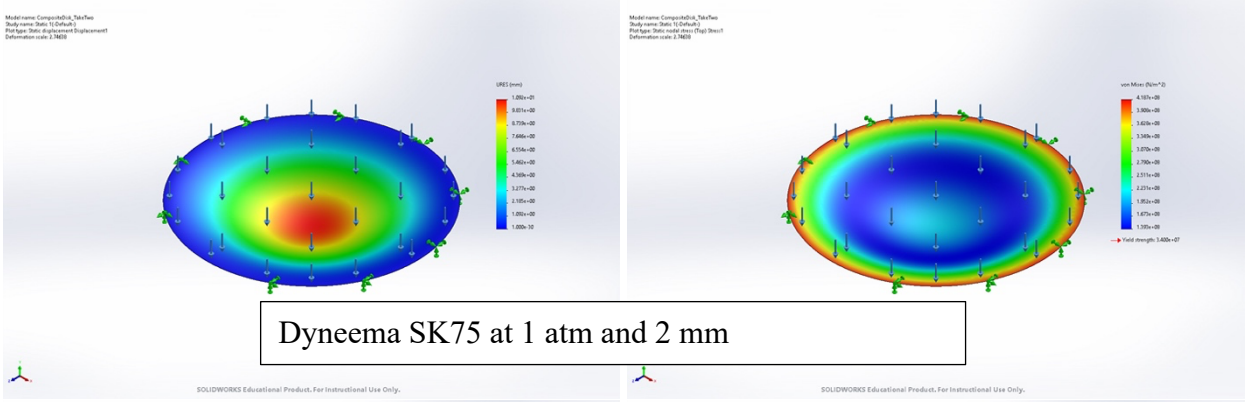

Dyneema SK75 at 1 atm and 2 mm

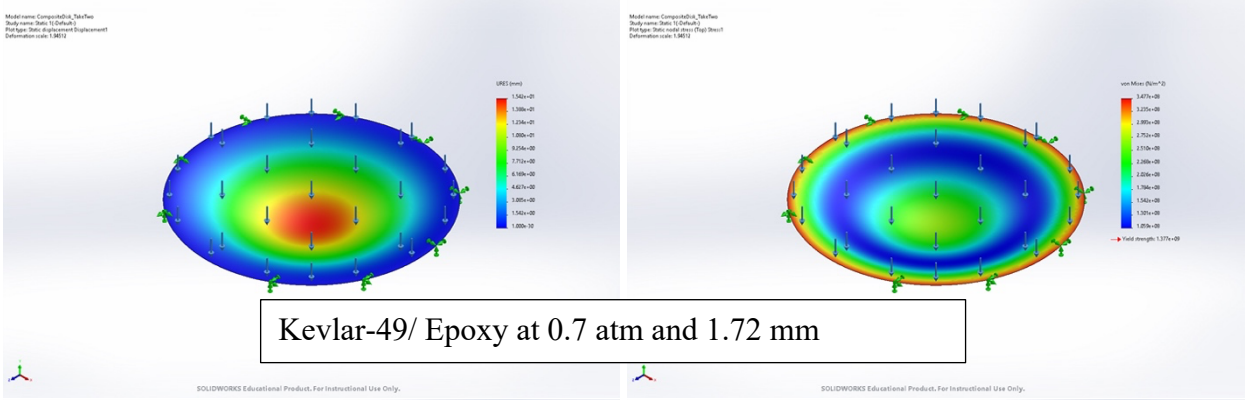

Kevlar-49/ Epoxy at 0.7 atm and 1.72 mm

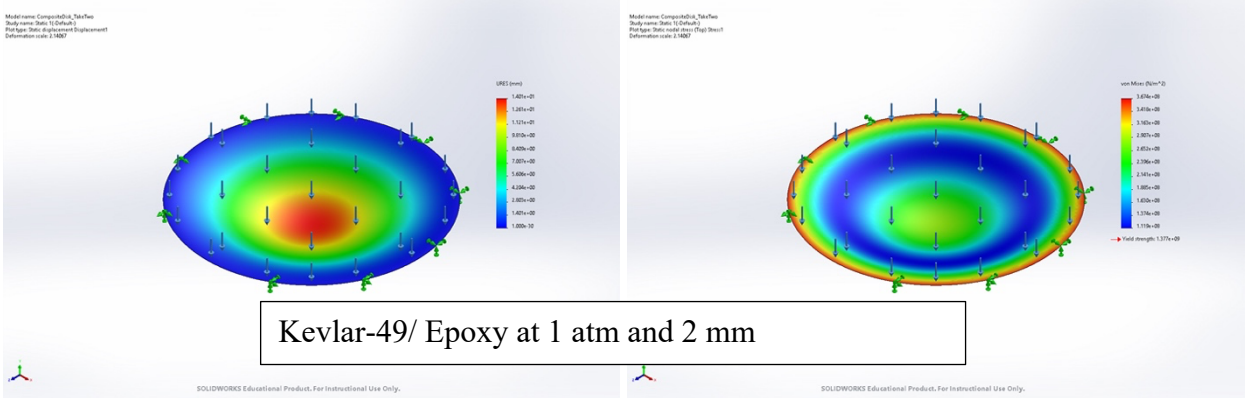

Kevlar-49/ Epoxy at 1 atm and 2 mm

REFERENCES

Adler, R., W. Albrecht, T. Alhalel, A. Angelopoulos, A. Apostolakis, E. Aslanides, G. Backenstoss, et al. "The CPLEAR Detector at CERN." *Nuclear Instruments and Methods in Physics Research Section A: Accelerators, Spectrometers, Detectors and Associated Equipment* 379, no. 1 (September 1996): 76–100. https://doi.org/10.1016/0168-9002(96)00542-6.

Amsc, N, and A AREA CMPS. "Composite Materials Handbook." *Polymer Matrix Composites Materials Usage, Design, and Analysis*, 2002.

Attwood, J.P., S.N. Khaderi, K. Karthikeyan, N.A. Fleck, M.R. O'Masta, H.N.G. Wadley, and V.S. Deshpande. "The Out-of-Plane Compressive Response of Dyneema® Composites." *Journal of the Mechanics and Physics of Solids* 70 (October 2014): 200–226. https://doi.org/10.1016/j.jmps.2014.05.017.

Azpitarte, Itxasne, Ana Zuzuarregui, Hayrensa Ablat, Leire Ruiz-Rubio, Alberto López-Ortega, Simon D. Elliott, and Mato Knez. "Suppressing the Thermal and Ultraviolet Sensitivity of Kevlar by Infiltration and Hybridization with ZnO." *Chemistry of Materials* 29, no. 23 (December 12, 2017): 10068–74. https://doi.org/10.1021/acs.chemmater.7b03747.

Choi, Ilbeom, Jin Gyu Kim, Dai Gil Lee, and Il Sung Seo. "Aramid/Epoxy Composites Sandwich Structures for Low-Observable Radomes." *Composites Science and Technology* 71, no. 14 (September 30, 2011): 1632–38. https://doi.org/10.1016/j.compscitech.2011.07.008.

D'Alessandro, G., A. Paiella, A. Coppolecchia, M.G. Castellano, I. Colantoni, P. de Bernardis, L. Lamagna, and S. Masi. "Ultra High Molecular Weight Polyethylene: Optical Features at Millimeter Wavelengths." *Infrared Physics & Technology* 90 (May 2018): 59–65. https://doi.org/10.1016/j.infrared.2018.02.008.

Datta, Rahul, David T. Chuss, Joseph Eimer, Thomas Essinger-Hileman, Natalie N. Gandilo, Kyle Helson, Alan J. Kogut, et al. "Anti-Reflection Coated Vacuum Window for the Primordial Inflation Polarization ExploreR (PIPER) Balloon-Borne Instrument." *Review of Scientific Instruments* 92, no. 3 (March 1, 2021): 035111. https://doi.org/10.1063/5.0029430.

DuPont. "KEVLAR® ARAMID FIBER TECHNICAL GUIDE." DuPont, 2017. https://www.dupont.com/content/dam/dupont/amer/us/en/safety/public/documents/en/Kevlar_Technical_Guide_0319.pdf.

Hauviller, C. "Design Rules for Vacuum Chambers," n.d., 12.

Janezic, M.D., and J.A. Jargon. "Complex Permittivity Determination from Propagation Constant Measurements." *IEEE Microwave and Guided Wave Letters* 9, no. 2 (February 1999): 76–78. https://doi.org/10.1109/75.755052.

Lamb, James. "Miscellaneous Data on Materials for Millimetre and Submillimetre Optics." *International Journal of Infrared and Millimeter Waves* 17 (December 1, 1996): 1997–2034. https://doi.org/10.1007/BF02069487.

Leonhardt, W J, and M Mapes. "DESIGN OF LARGE APERTURE, LOW MASS VACUUM WINDOWS," n.d., 4.

Parker Seal Group. *Parker O-Ring Handbook*. ORD 5700. Lexington, KY: Parker Seal Group, 1990. https://www.parker.com/Literature/O-Ring%20Division%20Literature/ORD%205700.pdf.

Pelton, E., and B. Munk. "A Streamlined Metallic Radome." *IEEE Transactions on Antennas and Propagation* 22, no. 6 (November 1974): 799–803. https://doi.org/10.1109/TAP.1974.1140896.

Shimizu, Y., H. Otsu, T. Kobayashi, T. Kubo, T. Motobayashi, H. Sato, and K. Yoneda. “Vacuum System for the SAMURAI Spectrometer.” *Nuclear Instruments and Methods in Physics Research Section B: Beam Interactions with Materials and Atoms* 317 (December 2013): 739–42. https://doi.org/10.1016/j.nimb.2013.08.051.

Speirs, Peter, Roco Molina, Elena Saenz, Paul Moseley Pavel Yagoubov, and Axel Murk. “Design and Measurement of Possible Wide-Band 67-116 GHz ALMA Vacuum Window Anti-Reflection Layers.” In *2020 14th European Conference on Antennas and Propagation (EuCAP)*, 1–5, 2020. https://doi.org/10.23919/EuCAP48036.2020.9135970.

Tanner, David, James A. Fitzgerald, and Brian R. Phillips. “The Kevlar Story—an Advanced Materials Case Study.” *Angewandte Chemie International Edition in English* 28, no. 5 (1989): 649–54. https://doi.org/10.1002/anie.198906491.

Torayca. *T300 Data Sheet*. Technical Data Sheet, CFA-001. Santa Ana, CA: Toray Carbon Fibers America, Inc, n.d. https://www.rockwestcomposites.com/media/wysiwyg/T300DataSheet_1.pdf.

Zoughi, Reza, and Brian Zonnefeld. “Permittivity Characteristics of Kevlar, Carbon Composites, E-Glass, and Rubber (33% Carbon) at X-Band (8–12 GHZ).” In *Review of Progress in Quantitative Nondestructive Evaluation*, edited by Donald O. Thompson and Dale E. Chimenti, 1431–36. Boston, MA: Springer US, 1991. https://doi.org/10.1007/978-1-4615-3742-7_38.